Double-Linker Sensitizer: Linker Interaction and Interfacial Electron Transfer

Han Yan,[†] Joseph P. Avenoso,[‡] Samantha Doble,[†] Ryan Harmer,[¶] Luis G. C. Rego,[*,§] Elena Galoppini,[*,¶] and Lars Gundlach[*,†,‡]

[†]*Department of Chemistry and Biochemistry, University of Delaware, Newark, Delaware 19716, United States*

[‡]*Department of Physics and Astronomy, University of Delaware, Newark, Delaware 19716, United States*

[¶]*Department of Chemistry, Rutgers University Newark, Newark, New Jersey 07102, United States*

[§]*Department of Physics, Universidade Federal de Santa Catarina, Florianópolis, SC 88040-900, Brazil*

E-mail: luis.gc.rego@gmail.com; galoppin@newark.rutgers.edu; larsg@udel.edu

Abstract

Interfacial electron transfer (IET) between novel perylene sensitizers substituted with double linkers, composed of a bridge and an anchor group, and TiO_2 was investigated by ultrafast spectroscopy and combined non-adiabatic quantum mechanical/-molecular dynamics (QM/MD) simulations. The influence of the linker substitution position on IET was investigated: one sensitizer was substituted with two acrylic acid linkers in peri position (pDtBuPe$(C_2H_2COOH)_2$, bis-peri) and another was substitute with two acrylic acid linkers in ortho position (oDtBuPe$(C_2H_2COOH)_2$, bis-ortho). For both double-linker sensitizers, MD calculations predicted that the molecules bind covalently with only one linker on the {101} surface of anatase TiO_2. The second linker

of the bis-peri binds via VdW interaction between the carboxyl anchor group of the acrylic acid linker and a pentacoordinated Ti^{4+} ion in the vicinity of the anchoring site, while the carboxyl anchor of the second bis-ortho linker forms a hydrogen bond with a 2-fold coordinated O_2^- ion on the {101} surface, away from the the anchoring site. Ultrafast transient absorption spectroscopy was performed to measure IET from the excited sensitizers and compared with IET from the single-linker derivatives of the sensitizers (pDtBuPeC_2H_2COOH, peri; oDtBuPeC_2H_2COOH, ortho). Experimental injection times agreed well with results from QM/MD simulations for both single and double linker molecules and supported a single-linker binding mode for the double-linker sensitizers. Comparison of IET times for the double-linker sensitizers with their single-linker variant showed unexpected variations. IET from bis-peri was significantly slower than from peri. Theory could explain this behavior by small changes in configuration due to steric interference between both linkers in peri position that have significant influence on IET rates. Principal component analysis was employed to identify the degrees of freedom that are most strongly correlated to variations in IET times. Furthermore, the influence of the substitution position (peri vs. ortho) on IET from single linker sensitizers was much smaller than the difference in the static electronic structure would imply. Comparison between bis-ortho and ortho, on the other hand, showed the expected result that the double-linker molecule injects faster than the single-linker variant. Finally, the strong effect of configurational changes on IET was also observed experimentally in modulation of IET due to coupling to vibrational modes, again, in excellent agreement with the QM/MD simulations.

Introduction

Light-induced interfacial electron transfer (IET) reactions from molecules to solids are central to a variety of energy related transport and conversion processes such as catalysis, photocatalysis, photovoltaics, energy storage, and molecular electronics.[1–6] The molecular sensitizers for each of these applications involves multiple components with different functionalities. A

molecular system for solar energy conversion by solar driven chemistry, for example, requires the formation of a stable interface, efficient light absorption, and charge transfer (CT) that promotes the desired reaction. For light driven CT processes, two components of the sensitizer molecule are essential: the core that adsorbs light, i.e. the chromophore, and the linker group that leads to a stable attachment of the chromophore to the surface. A lot of attention has been directed towards the chromophore, varying absorption spectra, and studying intramolecular relaxation pathways for applications in solar energy conversion.[4]

The linker is composed of an anchor group that attaches to the surface, and a bridge group the connects the anchor and the chromophore. Since an overwhelming amount of work involved TiO_2 interfaces, acidic anchor groups have been studied extensively.[7–9] In many cases, the linker group serves a second, very important role; it controls electronic coupling between the electron donor state on the chromophore and the acceptor states in the solid. Depending on its composition it can act as an IET promoting wire or as a barrier, and even rectifying behavior has been observed.[10,11] Recently, more focus has been set on investigating modifications of the bridge to alter the functionality of sensitized systems beyond their application in solar energy conversion. For example, bridges with a strong oriented dipole moment that gives control over the electronic level alignment have been investigated.[12] Molecular switching units have been investigated to gain control over functionality of sensitizers by external stimuli.[13] Several studies involved chromophores that were bound to TiO_2 via more than one anchor group[14,15] or where the chromophore itself was composed of several identical linkers.[16] Separating the two functions of the linkers by using one linker for stable chemical attachment to the surface and another linker-like unit that promotes interaction between the chromophore and the interface is an approach that gives more flexibility in designing the sensitizer and can add functionalities beyond IET. However, this approach has rarely been explored.

Heterogeneous IET systems have the advantages of a solid state structure. However, they introduce complications for computational and experimental investigations. Therefore,

model systems that are adapted to the experimental requirements as well as to theoretical treatment are essential to mitigate these challenges. Perylene based sensitizer have proven to be well suited for ultrafast spectroscopic investigations of IET, while still being accessible to combined non-adiabatic quantum mechanical/molecular dynamics simulations (QM/MD). Perylene TiO_2 systems have been used for numerous studies, experimental as well as computational.[7,17–21] Here, we study IET from a set of novel model sensitizers with two linkers in different substitution positions. While the sensitizers have two identical linkers, the binding mode is such that only one linker binds chemically via the carboxylic acid anchor group on the {101} surface of anatase while the other linker is only weakly coordinated with the surface via hydrogen bond or VdW interaction. This configuration is the simplest way to separate functionalities in multi-linker sensitizers. The double-linkers are substituted in different positions for comparing the influence of steric effects and effects of the static electronic structure of the chromophore on IET. IET is investigated in real time by femtosecond spectroscopy and compared to QM/MD simulations.

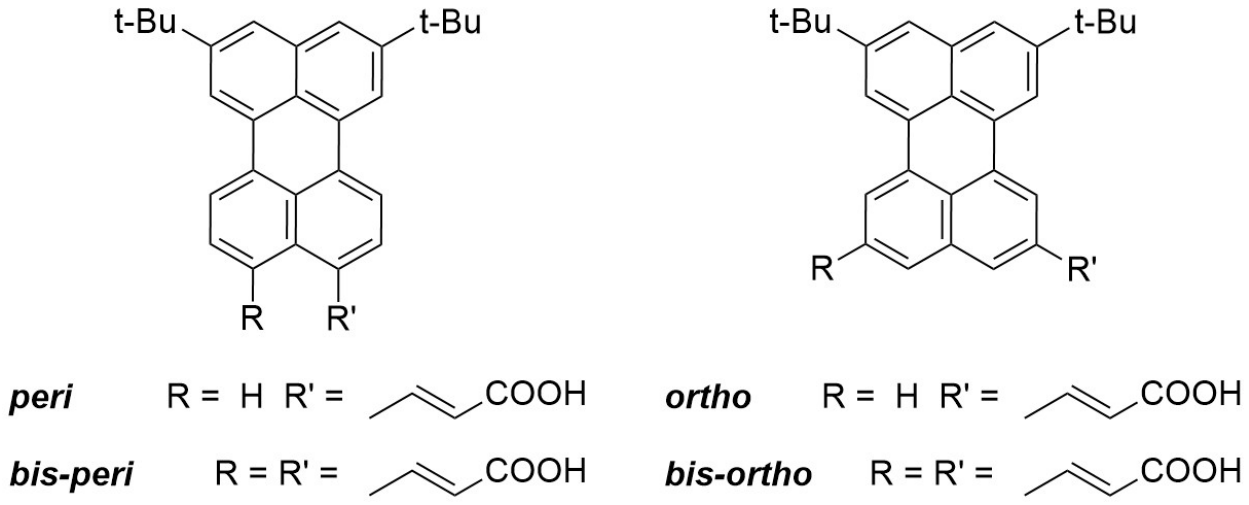

Figure 1: Molecular structure and abbreviations of the novel sensitizers investigated here. (E)-3-(8,11-Di-tert-butylperylen-3-yl)acrylic acid **[peri]**, (2E,2'E)-3,3'-(8,11-Di-tert-butylperylene-3,4-diyl)diacrylic acid **[bis-peri]** (E)-3-(8,11-Di-tert-butylperylen-2-yl)acrylic acid **[ortho]**, (2E,2'E)-3,3'-(8,11-Di-tert-butylperylene-2,5-diyl)diacrylic acid **[bis-ortho]**.[22]

Results and Discussion

The structure of the four sensitizers that were investigated, (E)-3-(8,11-Di-tert-butylperylen-2-yl)acrylic acid, (2E,2'E)-3,3'-(8,11-Di-tert-butylperylene-2,5-diyl)diacrylic acid, (E)-3-(8,11-Di-tert-butylperylen-3-yl)acrylic acid, (2E,2'E)-3,3'-(8,11-Di-tert-butylperylene-3,4-diyl)diacrylic acid are shown in Figure 1. They will be termed, ortho, bis-ortho, peri, and bis-peri, respectively, for the remainder of the article. The synthesis, the optical and electronic properties and QM simulations of the electronic structure of the sensitizer have been reported elsewhere.[22] Briefly, the substitutions had the expected effects on the electronic structure of the HOMO and LUMO frontier orbitals and on the spectral properties. A significant red-shift of 30 nm and 50 nm in ground state absorption was observed for the peri and bis-peri sensitizer, respectively. The two ortho substituted sensitizers showed a negligible red-shift of less than 7 nm with respect to the unsubstituted DtBuPe. The spectral shifts were consistent with TD-DFT calculations of the HOMO and LUMO and explained by a significant delocalization of the LUMO orbital over the linker groups in peri position, whereas the HOMO of the perylene core, i.e. the chromophore, was mostly unaffected by the substituted linkers. On the other hand, both frontier orbitals of the perylene core were only weakly affected by the substitution in ortho position. For ultrafast spectroscopic measurements of IET between the sensitizers and TiO_2, the sensitizers were adsorbed in 10 μm thick colloidal anatase TiO_2 films on thin glass substrates. The procedures for synthesizing collides, preparing the films, and film sensitization is described in the SI. The UV-vis difference spectra of the sensitizers on TiO_2 show a similar red-shift as in solution (Figure 2). While the blue edge of the spectra can be distorted by the subtraction of the strong TiO_2 absorption below 400 nm, the shift of the peak maximum is reliable. As expected, due to efficient IET into the film, the sensitized films did not show any fluorescence. This also confirms that the procedure for removal of unbound or weakly physisorbed sensitizers from the film is reliable (SI). Transient absorption (TA) measurements on the sensitized films were performed in high vacuum. The vacuum environment protects the sensitizers from photodegradation. Preventing photodegradation

is important since replenishment of the solid state sample is not possible and moving the sample to new spots during the measurement is not practical and would introduce noise. The vacuum environment also simplifies comparison to simulations on model systems.

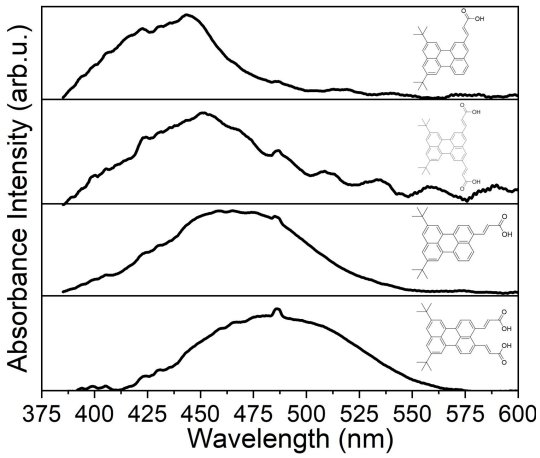

Figure 2: UV-vis difference spectra of ortho, bis-ortho, peri, and bis-peri adsorbed on colloidal TiO_2. The absorption of the unsensitized TiO_2 film is subtracted. Insert: Structure of the corresponding sensitizer molecules.

IET from differently substituted perylene chromophores, all in peri position, to TiO_2 has been investigated previously.[10,23] IET times ranged from around 12 fs for a directly bound carboxylic acid linker in peri position (Pe-COOH) to 100 fs for a saturated propionic acid linker in peri position. Therefore, a high time-resolution is required for the experiment. While pump pulses in the visible range can be generated with sub 10 fs FWHM, the length of the white-light pulse in a pump-probe TA measurement is restricted to around 20 fs. However, compensation of white-light chirp together with a global fitting procedure at different spectral positions allows us to reliably extract dynamics as fast as 12 fs from our measurements.[23] To exclude any uncertainty in the resolution of the TA measurements, we regularly perform control measurements on Pe-COOH that shows IET of 12 fs. The TA setup is described in detail in the SI.

TA maps of all four sensitizers at an excitation wavelength of 440 nm are shown in Figure 3. A systematic red-shift for both double-linker sensitizers is observed for the cation absorption, that is known to be located around 570 nm for the reference sensitizer, i.e. Pe-

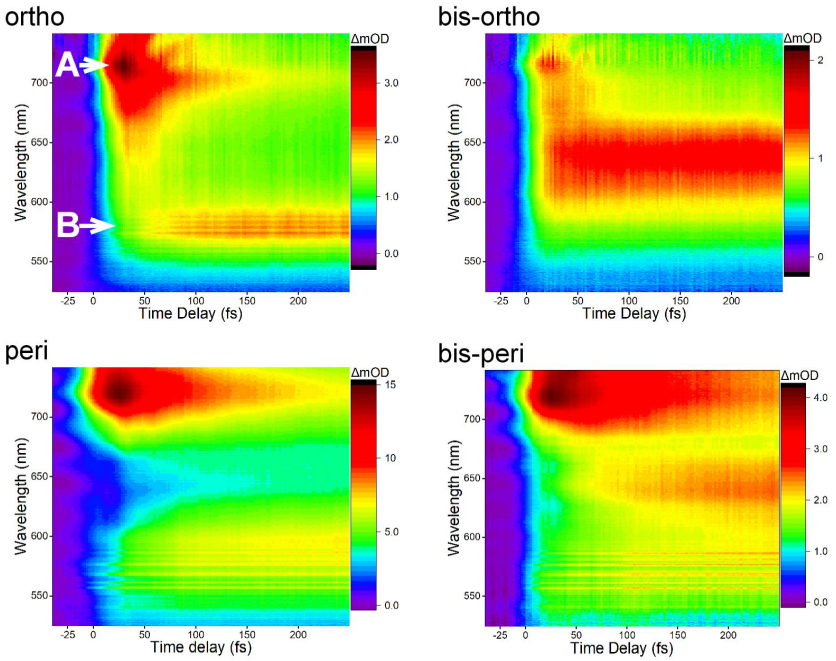

Figure 3: TA maps of the ortho, bis-ortho, peri, and bis-peri. The position of excited state absorption and cation absorption are indicated with arrows at A and B, respectively.

COOH. The excited state for the reference is located at around 720 nm. Since the spectral range in the experiment is limited to 750 nm by the white-light spectrum and the spectral range of the chirped mirrors (see SI), the extent of the red-shift for the excited state absorption in the peri substituted sensitizers cannot be quantified with certainty. It is interesting to note, that the excited state absorption shows the same trend as the ground state UV-vis spectrum where both peri substituted sensitizers are red shifted, while the cation absorption shows a red-shift for the double-linker sensitizers. In fact, DFT calculations, reported elsewhere,[22] show that the unoccupied virtual states are strongly stabilized as a result of single- and double-linker attachment in peri positions of the perylene molecule, in comparison to the reference Pe-COOH sensitizer. This effect is weaker for linkers substituted in ortho position. As mentioned above, injection times are extracted from these maps by fitting a two-level rate model simultaneously to the excited state and cation absorption transients. The model that includes the known pulse width and time-zero of the measurement. An example for such a fit is shown in Figure 4 for the ortho sensitizer. The black fit curves for the excited state

absorption (red dots), and the cation absorption (blue dots) are composed of contributions from excited state population (red solid) and cation population (blue solid line) to account for spectral overlap. The resulting injection times are summarized in table 1 together with computational results that will be discussed below.

Table 1: Comparison of experimental and computational electron transfer times for the 4 sensitizers.

	IET time (exp)	IET time (comp)
ortho	40 fs	28 fs
bis-ortho	17 fs	20 fs
peri	35 fs	13 fs
bis-peri	57 fs	25 fs

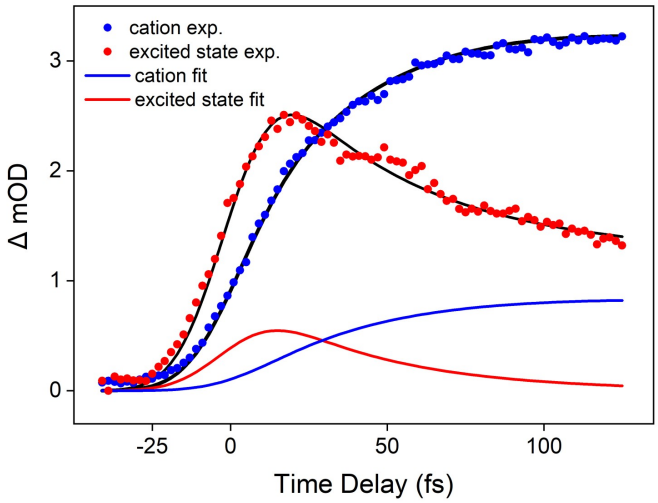

Figure 4: Excited state absorption (red), and cation absorption (blue) extracted at position A and B in the TA map in Figure 3. The contribution of the excited state population and the cation population to the fit curves is shown as red and blue solid line (not to scale).

Wavepacket modulated IET

The measurements for the peri and, in particular, the bis-peri cannot be fitted with the two-state model. As can be seen in Figure 5, the rise of the cation absorption signal shows a step-like modulation. To ensure that the modulation did not arise from artifacts, this result was reproduced on 6 different samples, including different batches of colloidal films, and in

21 individual measurements. Such dynamics have been observed in a small number of IET systems and can be explained by the formation of an electron wavepacket in the excited state of the sensitizer.[24–26]

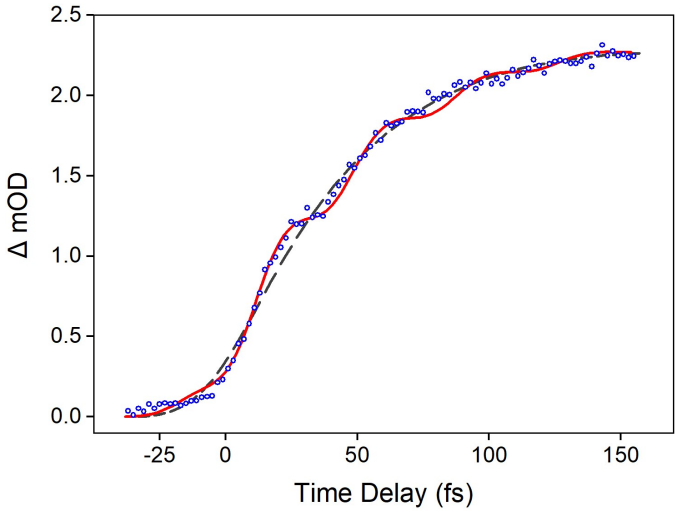

Figure 5: Rise of the transient cation absorption signal (blue dots). A fit to a two-level rate model is included as the black dashed line. The blue fit curve combines the two-level rate model with a harmonic step-like modulation.

The coherent wavepacket is triggered by the short excitation pulse. It modulates IET, giving rise to enhanced IET whenever the wavepacket approaches the crossing point between donor and acceptor potential energy surfaces (PESs). The formation of the wavepacket in peri substituted sensitizers and, in particular, its clear manifestation in the cation signal for bis-peri (Figure 5) can be explained by the red-shift of the sensitizers. Since the excitation wavelength for all sensitizers was identical, the peri, and to an even larger extent, the bis-peri were electronically excited in a higher vibrational state due to the red-shifted groundstate absorption. To reproduce the step-like rise in the cation signal, we modified the rate model with a harmonic modulation that accounts for wavepacket dynamic in the excited state. The phase of the modulation and the frequency were identical for all measurements and the frequency agrees very well with non-adiabatic MD simulations that show modulation of IET with 400 cm^{-1} for this system (vide infra). The step-like modulation complicates the assignment of an injection time from the rate model. While the simple rate model does not fit

the dynamics (black dashed line in Figure 5), the fit that includes the harmonic modulation is based on a phenomenological model and does not result in physically meaningful time constants. However, the injection time from the two-level rate model can be viewed as an average time-constant (c.f. black dashed and blue line in Figure 5). The assignment of the modulation to a vibrational wavepacket that is coherently excited and observed due to excess excitation energy can be confirmed by an experiment with smaller excitation energy. Figure S1 shows the same measurement as Figure 5 only at an excitation wavelength of 520 nm. At this excitation wavelength, no modulations were observed and the dynamics can be fitted globally with the two-level rate model and result in a 60 fs injection time. Hence, generation of a hot excited state can modulate IET, but does not change the overall time constant for IET. The difference of around 430 meV in excitation energy could in principle lead to coupling of the excited state to higher lying acceptor states in the TiO_2 conduction band. However, this effect does not change the injection time. A similar result has been found for a system where the molecular states were shifted by means of a surface dipole.[12] It should be noted, that the equivalent measurement with sufficient excess in excitation energy is not possible for the other three sensitizers because of the onset of interband absorption in TiO_2.

Comparison of injection times

The measured injection times do not match the intuitive expectation that, in general, a second linker should enhance electronic coupling and accelerate IET. Moreover, it is not expected to slow down IET, as observed in case of the bis-peri sensitizer. The ortho substituted sensitizers on the other hand showed the expected behavior, specifically, the bis-ortho showed more than two times faster IET compared to the ortho. It should be mentioned that IET from the peri sensitizer has been measured previously and a significantly faster injection time has been reported.[7] Therefore, utmost care was taken to confirm the results. As mentioned above, a sub-20 fs time resolution for the TA setup is confirmed before each

measurement with the reference compound Pe-COOH. In addition, the measurements were repeated on 5 different samples during a time period of several weeks on different batches of TiO_2 film. The 35 fs injection time for the peri was reproduced in a total of 35 individual measurements. The main difference between the measurements that were previously reported and the ones presented here, is that previously single color pump-probe spectroscopy was employed. Single color pump-probe spectroscopy does not simultaneously record dynamics of excited state and cation absorption, and only the cation absorption dynamics was measured and evaluated. The discussion of the injection dynamics depends on the knowledge of the binding mode, specifically whether the double-linker molecules bind with both linkers and if both anchor groups result in the same binding. It is challenging to address this question experimentally. While, in some cases IR spectroscopy has been employed to monitor the disappearance of the C=O stretch mode of the carboxylic acid anchor upon binding to TiO_2,[14,27] IR and Raman did not give definite results in case of the double-linker molecules investigated here.

Therefore, possible configurations of the sensitizers on the anatase {101} surface were modeled for evaluating the binding mode and geometry. Initially, the geometry of the molecules was optimized using density functional theory (DFT) in gas phase at the B3LYP/6-31+G(d,p) level and their electronic properties were obtained at the CAM-B3LYP/6-31+G(d) level. The calculations were carried out using the Gaussian 09 package. To accelerate the calculations, simplified model compounds, in which the bulky tert-butyl groups (DiBuPe) were substituted by methyl groups (DiMePe), were used. It was verified, both in static and dynamics calculations, that this substitution did not induce significant changes to the results (vide supra). The DFT results were then used as a reference to parametrize a semi-empirical extended Hückel (eH) model upon which the coupled charge transfer/non-adiabatic molecular dynamics simulations were carried out. Details of the procedure are described in previous publications,[28,29] including the parameterization of the eH model.[23] The sensitizer/TiO_2 interface model systems consist of the sensitizer molecules bound to the {101} surface of

anatase TiO_2 by the carboxyl group in a bidentate bridging geometry. This prototypical bidentate bridging geometry provides stability against water and robust electronic coupling between sensitizer and substrate.[20,30,31] The surface of anatase colloids consist predominantly of {101} faces, as reported in experimental[24] and theoretical[32] studies. In fact, DFT total energy calculations together with the Wulff construction method show that for anatase crystals the most stable {101} face constitutes more than 90% of the exposed crystal surface. Several binding configurations of the four sensitizers to the anatase cluster were investigated. Figure 6a)-f) shows frames of the sensitizer/interface system captured at intervals of 4 picoseconds during a MM simulation over 100 ps at 300 K.

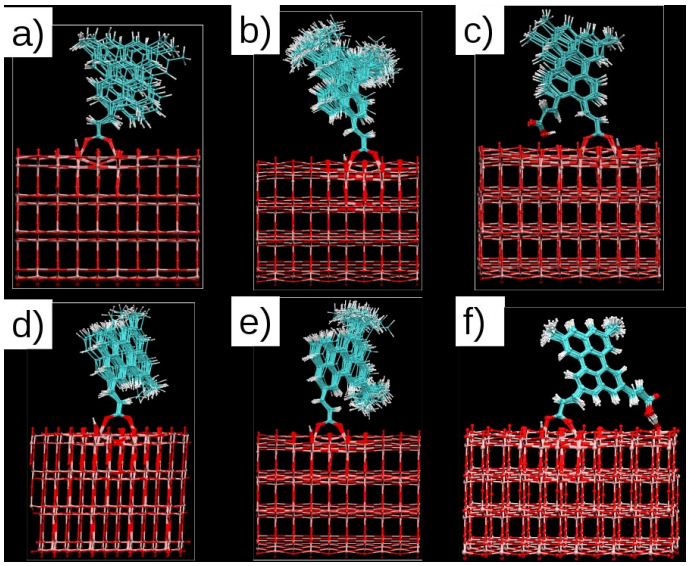

Figure 6: Frames of the sensitizer/interface system captured at 4 picoseconds intervals during a MM simulation over 100 ps at 300 K. a) peri-DiMePe, b) peri-DiBuPe, c) bis-peri-DiMePe, d) ortho-DiMePe, e) ortho-DiBuPe, f) bis-ortho-DiMePe.

The simulations showed that for the double-linker sensitizers, just one of the linkers is chemically attached to the anatase surface in the bridging bidentate geometry. The second linker is connected to the surface by long range Coulomb interactions between the oxygen atoms of the COOH group and a pentacoordinated Ti^{4+} ion of the surface, c.f. left linker in Figure 6c), or by a hydrogen bond formed between the carboxylic group and a 2-fold coordinated O_2^- ion, c.f. right linker in Figure 6f). Both intermolecular bonds provide

dynamic stability to the sensitizer. The simultaneous covalent bonding of both linkers was excluded because it generates considerable strain on the sensitizer due to unreasonable torsion angles. Therefore, these configurations carry a large energy penalty.

Following the definition of the models for the sensitizer molecules on the anatase surface we simulated IET dynamics. In the model system, all nuclei comprising the sensitizer molecule as well as the nuclei of the TiO_2 cluster in the vicinity of the anchoring site (varying from 11 to 13 TiO_2 units) were free to move in the MD simulation. The other nuclei of the TiO_2 cluster remained constrained to their optimized positions during classical and excited-state non-adiabatic dynamics. For modeling IET, though, all atoms of the sensitizer/TiO_2 system, free and constrained, were treated quantum mechanically.

Next, we analyzed the effect of the molecular configuration on the IET times by taking 100 configurations at intervals of 1 ps from the MD simulation. These molecular configurations – some of them shown in Figure 6 – are used as initial condition for the electron transfer dynamics simulation shown in Figure 7.

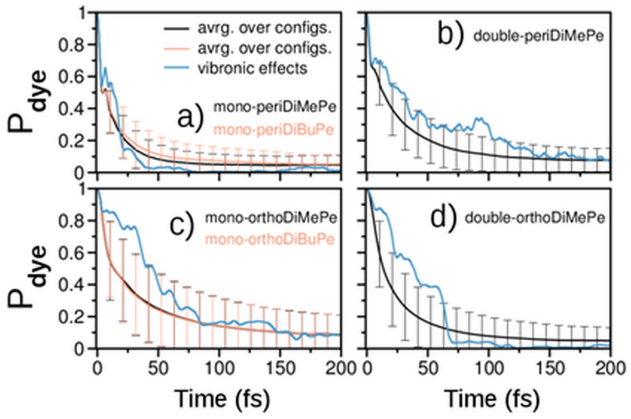

Figure 7: Interfacial electron transfer dynamics for a) peri, b) bis-peri, c) ortho, and d) bis-ortho. Error bars represent the time-dependent variance of IET curves averaged over 100 initial configurations: black curves correspond to DiMePe molecules and red curves to DiBuPe model sensitizers, refer to Figure 6 for details of the structure. Blue curve describes IET dynamics including vibronic effects.

In the configuration-averaged IET calculations the nuclei are maintained fixed during the simulation. The survival probabilities, P_s were averaged over 100 individual simulations

and the resulting variance was calculated as a function of time (error bars in Figure 7). The results are shown in Figure 7a)-d). The black curves are simulations of the simplified DiMePe sensitizers and the red curves show the comparison with the full DiBuPe sensitizers with the linkers in ortho position. There are negligible differences between the average IET curves for the peri DiMePe and DiBuPe, suggesting that the bulky di-tert-butyl groups, that are used in the experiment to prevent intermolecular interactions, not only have very little influence on the frontier orbitals of perylene[22] but also do not influence the molecular dynamics of the attached sensitizers significantly. Therefore, further calculations were performed with the DiMePe sensitizers. As can be seen in Figure 7, there is considerable variance in the IET dynamics for individual structural configurations, indicating the sensitivity of the perylene/TiO_2 electronic coupling to the perylene/C_2H_2-bridge mutual geometry. The simulated injection times (mono-exponential fits to the black curves in Figure 7) are listed in table 1. The overall agreement with the experiment is very good and shows the same trend for the four sensitizers. However, theory systematically predicts faster IET times than observed in the experiments. The discrepancy may be caused by the fact that the configuration-averaged IET times are obtained by calculations with static nuclei. Including vibrational relaxation effects in the present IET simulations by the non-adiabatic molecular dynamics tends to delay IET. The results are shown as blue lines in Figure 7a)-d). These results correspond to a single trajectory. The initial conditions are the same as for the first frame that was used to calculate the configuration-averaged IET dynamics. The non-adiabatic charge transfer dynamics, including vibronic effects, leads to a delay in the initial electron injection into the TiO_2 for all four sensitizers. This behavior can be understood by analyzing the intramolecular reorganization dynamics in the sensitizer upon excitation to the S_1 state.

Figure 8 illustrates the essential concurrent effects that take place upon the photoexcitation: excitation of vibrational normal modes; relaxation of vibrational energy and intramolecular reorganization; and electron transfer from the S1 state of the sensitizer to the

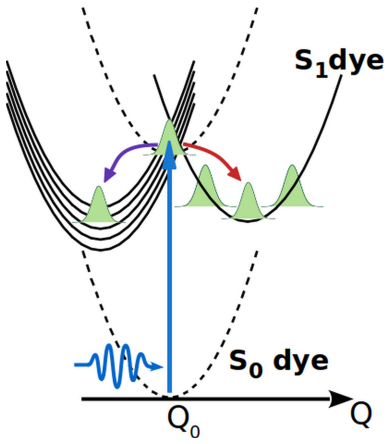

Figure 8: The upper part illustrates the excitation of vibrational normal modes due to photoexcitation to the S_1 state in the bis-peri sensitizer and two competing dynamic processes: intramolecular relaxation (red arrow) and electron transfer to the semiconductor bands (purple arrow).

conduction band of the semiconductor. Luis: Do we want to put this back into Fig.8? The lower part shows the electron-hole pair difference energy, defined as the difference between the energies of the photoexcited electron and hole, obtained by non-adiabatic dynamics simulations for the bis-peri molecule in gas phase (blue) and for the corresponding sensitizer/TiO_2 system (orange). The initial wavepacket dynamics (orange) reduces periodically the e-h energy substantially in the first 25 fs. This reduction in energy drives the donor state out of resonance with the acceptor states in the simulation and impedes electron transfer.

The Fourier transformation of the oscillations in the e-h excitation energy shows three main peaks (Figure S3): a small peak around 420 cm^{-1} that is ascribed to the perylene ring breathing and deformation modes, and two strong peaks at 1620 cm^{-1} and 2020 cm^{-1}, that are both connected to local C=C stretching as well as perylene ring stretching modes. The 420 cm^{-1} mode matches very well with the period of the step-wise modulation in the cation signal in Figure 5 and supports that IET is modulated by the formation of an electronic wavepacket in this case. The two high frequency modes with periods below 20 fs cannot be observed experimentally in white-light TA because of the limited time resolution. The simulated HET dynamics suggests that electron transfer occurs mainly through just one of

the linkers in the double-linker molecules, since the presence of a second linker does not significantly accelerate the electron injection for the bis-ortho sensitizer and slows it down for the bis-peri In the simulations. This is confirmed by Figure 9 that shows snapshots of the photoexcited electron density at different times as it is injected into TiO_2. The snapshots at 10 fs and 20 fs show clearly that IET occurs predominantly through the linker that is covalently bound to the surface. This can explain why, in the simulations, the second linker for the otho substituted sensitizers only slightly decreases IET time from 28 fs to 20 fs. The fact that the experimental difference is bigger (40 fs vs. 17 fs, respectively) suggest that edges and defects on a real surface allow a subset of sensitizers to bind with both linkers.

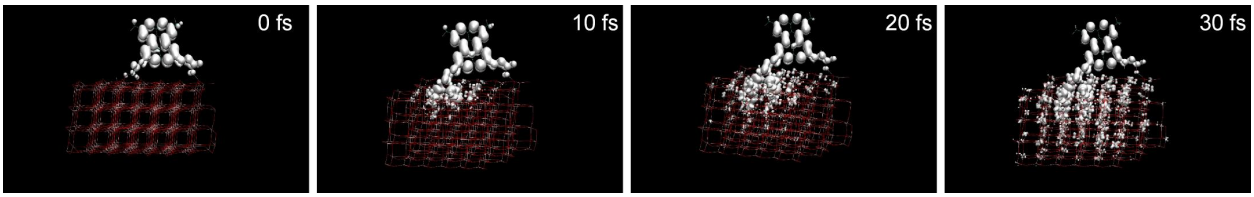

Figure 9: Snapshots of the electron density of the electron during injection into TiO_2 at different times after excitation.

Steric effects on electron transfer

The question remains why the bis-peri showed much slower IET time than the peri sensitizer, experimentally (57 fs vs. 35 fs) as well as theoretically (25 fs vs. 13 fs). For gaining insight into the effect of the second loosely bound linker (LL) in the bis-peri sensitizer on IET, we investigated steric effects during IET. The effect of the interaction between both linkers on IET can be associated to a number of degrees of freedom indicated in 10: the rotation of the linkers (blue arrows), the dihidral angle between the linkers (green arrow), the distance between the H atoms on the linkers (red double arrow), and the distance between the weakly bound COOH group and the nearest Ti atom on the surface (pink double arrow). The random nature of generating specific configurations in individual frames complicates the systematic identification of the the most relevant parameters. To identify correlations

between the different degrees of freedom and the IET times, principal component analysis was employed. Luis: I guess we have to see what we get out of it

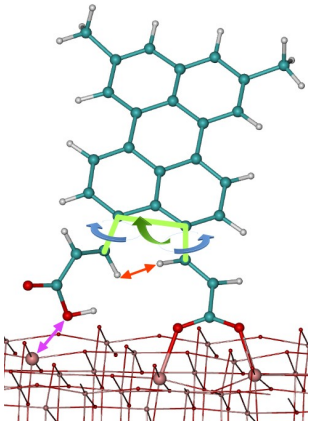

Figure 10: Scheme of the molecular degrees of freedoms that have strong influence on electronic coupling; blue arrows: rotation of the linkers, green arrow: dihidral angle between the linkers, red double arrow: distance between the H atoms on the linkers, pink double arrow: distance between the weakly bound COOH group and the nearest Ti atom on the surface.

Conclusions

A set of new model sensitizer molecules was employed to study light induced IET from double-linker sensitizers to TiO_2, with a focus on the influence of non-equivalent linkers on electron transfer dynamics. Comparison between sensitizers equipped with one linker and with two linkers showed unexpected sensitivity of IET times on linker configuration. Theory showed that the double-linker sensitizers bind covalently only with one linker, while the other linker is only weakly associated with the TiO_2 surface. Overall, calculated IET times agree well with the measurements and show the same trends. Vibronic effects that have been observed experimentally match very well with simulations that show a modulation of the e-h energy with a 440 cm^{-1} mode. Moreover, theory could explain the surprising slow-down in IET for a double-linker sensitizer and showed that steric effects between the two linkers lead to a distortion of the perylene core, to enhanced delocalization of the excited electron over the second leg, and to reduced electronic coupling. The effect of this steric distortion on IET is stronger than the effect of different substitution sites (ortho vs. peri). This study

emphasizes that the often neglected coupling of electronic and nuclear/vibrational degrees of freedom can influence charge carrier dynamics more strongly than static electronic effects.

Acknowledgement

For the financial support the authors are thankful to the U.S. Department of Energy, Office of Science, Office of Basic Energy Sciences, Office of Solar Energy Research, under Awards Number DE-FG02-01ER15256 (Galoppini) and DESC0016288 (Gundlach)); Duke University and CNPq/Brazil and the National Laboratory for Scientific Computing (LNCC/MCTI, Brazil), and FAPESC-H2020-MSCA-RISE-2017 (OCTA, #778158) (Rego). Elena Galoppini is grateful to Rutgers University for a sabbatical leave and Ryan Harmer is grateful to Prof. Piotr Piotrowiak and Dr. Yaroslav Aulin (Rutgers Newark) for their assistance with lifetime and quantum yield measurements. Luis G.C. Rego would like to express gratitude for Duke University and CNPq/Brazil for support during a sabbatical leave, the National Laboratory for Scientific Computing (LNCC/MCTI, Brazil), and FAPESC-H2020-MSCA-RISE-2017 (OCTA, #778158).

Supporting Information Available

The Supporting Information is available free of charge at https://pubs.acs.org/doi/ Figures S1 - S..., experimental methods, kinetics fitting, computational methods Tables S... (PDF)

References

(1) Park, H.; il Kim, H.; hee Moon, G.; Choi, W. Photoinduced charge transfer processes in solar photocatalysis based on modified TiO2. *Energy & Environmental Science* **2016**, *9*, 411–433.

(2) Esswein, A. J.; Nocera, D. G. Hydrogen Production by Molecular Photocatalysis. *Chem. Rev.* **2007**, *107*, 4022–4047.

(3) Ashford, D. L.; Gish, M. K.; Vannucci, A. K.; Brennaman, M. K.; Templeton, J. L.; Papanikolas, J. M.; Meyer, T. J. Molecular Chromophore–Catalyst Assemblies for Solar Fuel Applications. *Chem. Rev.* **2015**, *115*, 13006–13049.

(4) Hagfeldt, A.; Boschloo, G.; Sun, L.; Kloo, L.; Pettersson, H. Dye-Sensitized Solar Cells. *Chem. Rev.* **2010**, *110*, 6595–6663.

(5) Youngblood, W. J.; Lee, S.-H. A.; Maeda, K.; Mallouk, T. E. Visible Light Water Splitting Using Dye-Sensitized Oxide Semiconductors. *Acc. Chem. Res.* **2009**, *42*, 1966–1973.

(6) Hu, K.; Sampaio, R. N.; Schneider, J.; Troian-Gautier, L.; Meyer, G. J. Perspectives on Dye Sensitization of Nanocrystalline Mesoporous Thin Films. *J. Am. Chem. Soc.* **2020**, *142*, 16099–16116.

(7) Ernstorfer, R.; Gundlach, L.; Felber, S.; Storck, W.; Eichberger, R.; Willig, F. Role of Molecular Anchor Groups in Molecule-to-Semiconductor Electron Transfer†. *The Journal of Physical Chemistry B* **2006**, *110*, 25383–25391.

(8) Ambrosio, F.; Martsinovich, N.; Troisi, A. What Is the Best Anchoring Group for a Dye in a Dye-Sensitized Solar Cell? *The Journal of Physical Chemistry Letters* **2012**, *3*, 1531–1535.

(9) Galoppini, E. Linkers for Anchoring Sensitizers to Semiconductor Nanoparticles. *Coord. Chem. Rev.* **2004**, *248*, 1283–1297.

(10) Gundlach, L.; Ernstorfer, R.; Willig, F. Ultrafast interfacial electron transfer from the excited state of anchored molecules into a semiconductor. *Prog. Surf. Sci.* **2007**, *82*, 355–377.

(11) Jiang, J.; Swierk, J. R.; Hedström, S.; Matula, A. J.; Crabtree, R. H.; Batista, V. S.; Schmuttenmaer, C. A.; Brudvig, G. W. Molecular design of light-harvesting photosensitizers: effect of varied linker conjugation on interfacial electron transfer. *Phys. Chem. Chem. Phys.* **2016**, *18*, 18678–18682.

(12) Nieto-Pescador, J.; Abraham, B.; Li, J.; Batarseh, A.; Bartynski, R. A.; Galoppini, E.; Gundlach, L. Heterogeneous Electron-Transfer Dynamics through Dipole-Bridge Groups. *The Journal of Physical Chemistry C* **2015**, *120*, 48–55.

(13) Tegeder, P. Optically and thermally induced molecular switching processes at metal surfaces. *Journal of Physics: Condensed Matter* **2012**, *24*, 394001.

(14) Rochford, J.; Galoppini, E. Zinc(II) Tetraarylporphyrins Anchored to TiO_2, ZnO, and ZrO_2 Nanoparticle Films through Rigid-Rod Linkers. *Langmuir* **2008**, *24*, 5366–5374.

(15) Shahroosvand, H.; Abbasi, P.; Bideh, B. N. Dye-Sensitized Solar Cell Based on Novel Star-Shaped Ruthenium Polypyridyl Sensitizer: New Insight into the Relationship between Molecular Designing and Its Outstanding Charge Carrier Dynamics. *ChemistrySelect* **2018**, *3*, 6821–6829.

(16) Urbani, M.; Barea, E. M.; Trevisan, R.; Aljarilla, A.; de la Cruz, P.; Bisquert, J.; Langa, F. A star-shaped sensitizer based on thienylenevinylene for dye-sensitized solar cells. *Tetrahedron Lett.* **2013**, *54*, 431–435.

(17) Asbury, J. B.; Hao, E.; Wang, Y.; Ghosh, H. N.; Lian, T. Ultrafast Electron Transfer Dynamics from Molecular Adsorbates to Semiconductor Nanocrystalline Thin Films. *The Journal of Physical Chemistry B* **2001**, *105*, 4545–4557.

(18) Gundlach, L.; Burfeindt, B.; Mahrt, J.; Willig, F. Dynamics of ultrafast photoinduced heterogeneous electron transfer, implications for recent solar energy conversion scenarios. *Chem. Phys. Lett.* **2012**, *545*, 35–39.

(19) Gundlach, L.; Letzig, T.; Willig, F. Test of Theoretical Models for Ultrafast Heterogeneous Electron Transfer with Femtosecond Two-Photon Photoemission Data. *Journal of Chem. Sci.s* **2009**, *121*, 561–574.

(20) Persson, P.; Lundqvist, M. J.; Ernstorfer, R.; Goddard, W. A.; Willig, F. Quantum Chemical Calculations of the Influence of Anchor-Cum-Spacer Groups on Femtosecond Electron Transfer Times in Dye-Sensitized Semiconductor Nanocrystals. *J. Chem. Theory Comput.* **2006**, *2*, 441–451.

(21) Burfeindt, B.; Hannappel, T.; Storck, W.; Willig, F. Measurement of Temperature-Independent Femtosecond Interfacial Electron Transfer from an Anchored Molecular Electron Donor to a Semiconductor as Acceptor. *J. Phys. Chem.* **1996**, *100*, 16463–16465.

(22) Harmer, R.; Fan, H.; Lloyd, K.; Doble, S.; Avenoso, J.; Yan, H.; Rego, L. G. C.; Gundlach, L.; Galoppini, E. Synthesis and Properties of Perylene-Bridge-Anchor Chromophoric Compounds. *J. Phys. Chem. A* **2020**, *124*, 6330–6343.

(23) Oliboni, R. S.; Yan, H.; Fan, H.; Abraham, B.; Avenoso, J. P.; Galoppini, E.; Batista, V. S.; Gundlach, L.; Rego, L. G. C. Vibronic Effects in the Ultrafast Interfacial Electron Transfer of Perylene-Sensitized TiO_2 Surfaces. *J. Phys. Chem. C* **2019**, *123*, 12599–12607.

(24) Zimmermann, C.; Willig, F.; Ramakrishna, S. S.; Burfeindt, B.; Pettinger, B.; Eichberger, R.; Storck, W. Experimental Fingerprints of Vibrational Wave-Packet Motion During Ultrafast Heterogeneous Electron Transfer. *J. Phys. Chem. B* **2001**, *105*, 9245–9253.

(25) Huber, R.; Moser, J.-E.; Grätzel, M.; Wachtveitl, J. Real-Time Observation of Photoinduced Adiabatic Electron Transfer in Strongly Coupled Dye/Semiconductor Colloidal Systems with a 6 fs Time Constant. *J. Phys. Chem. B* **2002**, *106*, 6494–6499.

(26) Huber, R.; Dworak, L.; Moser, J. E.; Grätzel, M.; Wachtveitl, J. Beyond Vibrationally Mediated Electron Transfer: Coherent Phenomena Induced by Ultrafast Charge Separation. *J. Phys. Chem. C* **2016**, *120*, 8534–8539.

(27) Chen, Y.; Zhang, Q.; Flach, C.; Mendelsohn, R.; Galoppini, E.; Reyes, P. I.; Yang, K.; Li, R.; Li, G.; Lu, Y. Functionalization of MgZnO nanorod films and characterization by FTIR microscopic imaging. *Anal. Bioanal.Chem.* **2017**, *409*, 6379–6386.

(28) Oliboni, R. S.; Bortolini, G.; Torres, A.; Rego, L. G. C. A Nonadiabatic Excited State Molecular Mechanics/Extended Hückel Ehrenfest Method. *J. Phys. Chem. C* **2016**, *120*, 27688–27698.

(29) Rego, L. G. C.; Bortolini, G. Modulating the Photoisomerization Mechanism of Semiconductor-Bound Azobenzene-Functionalized Compounds. *J. Phys. Chem. C* **2019**, *123*, 5692–5698.

(30) Vittadini, A.; Selloni, A.; Rotzinger, F. P.; Grätzel, M. Formic Acid Adsorption on Dry and Hydrated TiO_2 Anatase (101) Surfaces by DFT Calculations. *J. Phys. Chem. B* **2000**, *104*, 1300–1306.

(31) Ikäläinen, S.; Laasonen, K. A DFT study of adsorption of perylene on clean and altered anatase (101) TiO_2. *Phys. Chem. Chem. Phys.* **2013**, *15*, 11673.

(32) Lazzeri, M.; Vittadini, A.; Selloni, A. Structure and energetics of stoichiometric TiO_2 anatase surfaces. *Phys. Rev. B* **2001**, *63*.

Graphical TOC Entry

Some journals require a graphical entry for the Table of Contents. This should be laid out "print ready" so that the sizing of the text is correct.
Inside the `tocentry` environment, the font used is Helvetica 8 pt, as required by *Journal of the American Chemical Society*.
The surrounding frame is 9 cm by 3.5 cm, which is the maximum permitted for *Journal of the American Chemical Society* graphical table of content entries. The box will not resize if the content is too big: instead it will overflow the edge of the box.
This box and the associated title will always be printed on a separate page at the end of the document.